Ytterbium Fiber Laser Based on a Three Beam Optical Path Mach–Zehnder Interferometer

Arturo Castillo-Guzman, Juan M. Sierra-Hernandez, Romeo Selvas-Aguilar, Daniel Toral-Acosta, Everardo Vargas-Rodriguez, Eloisa Gallegos-Arellano, Miguel Torres-Cisneros, Maria S. Avila-Garcia, and Roberto Rojas-Laguna

***Abstract*— In this letter, a switchable ytterbium doped double cladding photonic crystal fiber (Yb-doped-DCPCF) laser based on a three optical path Mach–Zehnder interferometer (MZI) is presented. Here, the MZI with three-beam path was achieved by fusion splicing a segment of an Yb-doped-DCPCF between two pieces of single mode fibers. Moreover, in the proposed laser arrangement, the Yb-doped-DCPCF segment is acting simultaneously as the MZI and also as the gain medium. This laser can be switched to emit a single or double line by controlling the polarization state and it operates within the range from 1028 to 1033 nm. In addition, the laser emission has a linewidth of 0.07 nm and a single-mode suppression ratio of 40 dB. Finally, it is shown that the fiber laser arrangement is compact and robust and that requires a relativity simple fabrication procedure.**

***Index Terms*— Photonic crystal fiber, fiber optics lasers, Mach-Zehnder interferometer.**

I. Introduction

In RECENT years, ytterbium doped fiber lasers (Yb-doped-FLs) have been studied since these have interesting characteristics such as simple energy level and excellent Yb-ion power conversion efficiency [1]. Because of these properties Yb-doped-FLs are attractive devices for very different applications such as material processing, spectroscopy, fiber optic sensors, ultrafast pulse generation and optical instrument testing [2]–[6]. Several configurations of Yb-doped-FLs are based on wavelength selective filters (WSF), since these make possible to control the laser emission line position [7]–[15]. These type of filters can be implemented by using different techniques, for instance by using non-linear polarization rotation plates [7], Sagnac loop mirrors [8], [9], fiber Bragg gratings (FBG) [10] and Mach-Zehnder interferometers [11]–[15]. Among them, MZI are particularly attractive for Yb-doped-FL applications since usually these have a simple configuration and high sensitivity. In fact, in the literature, a large number of Yb-doped-FLs based on a MZI can be found. For instance, the Yb-doped-FL proposed by [11], where the MZI was performed by splicing two couplers in cascade and was able to emit four lines. Tu *et al.* [12] proposed a tunable Yb-doped-FL, with a range of emission from 1040 to 1048 nm, which was based on a MZI manufactured in cascade by two couplers. Another case of multiline Yb-doped-FL was demonstrated by [13], in which by splicing two thermally expanded core fibers in cascaded a MZI was achieved. Another example of an Yb-doped-FL is the one proposed by Moghaddam *et al.* [14], where the MZI was based on a Sagnac loop mirror, which has a tuning range from 1030 to 1050 nm. Recently, a tunable double-clad ytterbium-doped fiber laser based on a double-pass MZI was presented and demonstrated by [15], in which the laser is adjustable over the range from 1064 to 1104 nm. Here, it is important to point out that all these lasers use the gain medium and the MZI as two different and independent components. Hence, in this work, an Yb-doped-DCPCF laser based on a type of three beam path Mach-Zehnder is presented. Moreover, in this arrangement the Yb-doped-DCPCF acts simultaneously as the MZI and also as the source gain medium. Finally, it is shown that this laser can be switched between one and two line emissions by controlling the polarization state and operates within the range from 1028 to 1033 nm.

Manuscript received March 19, 2016; revised June 6, 2016 and July 8, 2016; accepted October 1, 2016. Date of publication October 12, 2016; date of current version November 4, 2016. This work was supported by the National Council for the Science and Technology of Mexico under Project 183893. The work of M. S. Avila-Garcia was supported by the National Council for the Science and Technology of Mexico under Program 243981.

A. Castillo-Guzman, R. Selvas-Aguilar, and D. Toral-Acosta are with the Facultad de Ciencias Fisico Matematicas, Universidad Autonoma de Nuevo Leon, San Nicolas de los Garza 66451, Mexico.

J. M. Sierra-Hernandez, M. Torres-Cisneros, and R. Rojas-Laguna are with the Departamento de Ingenieria Electronica, Campus Irapuato-Salamanca, Universidad de Guanajuato, Salamanca, Mexico (e-mail: jm.sierrahernandez@ugto.mx).

E. Vargas-Rodriguez, E. Gallegos-Arellano, and M. S. Avila-Garcia are with the Departamento de Estudios Multidisciplinarios, Universidad de Guanajuato, Mexico.

Color versions of one or more of the figures in this letter are available online at http://ieeexplore.ieee.org.

Digital Object Identifier 10.1109/LPT.2016.2616466

II. MZI Fabrication and Principle Operation

Given that in the proposed setup an Yb-doped-DCPCF acts both as a gain medium and as a MZI filter, it is important to determine its optimum length. Experimental fluorescence characterizations of Yb-doped-DCPCF at pumping power values were realized and showed that a length of 60 cm gives an optimal amplified spontaneous emission [14]. Hence, the fabrication of the three beam optical path MZI filter consists in splicing 60 cm of Yb-doped-DCPCF (model HD699) between two SMFs segments (Fig. 1a). The Yb-doped-DCPCF has a 550 ppm by weight Yb^{3+} core with diameter of 9 μm (n_1), an inner cladding of 36 μm (n_2), numerical aperture of 0.08, cutoff wavelength 940 nm, air hole diameter of 10μm with

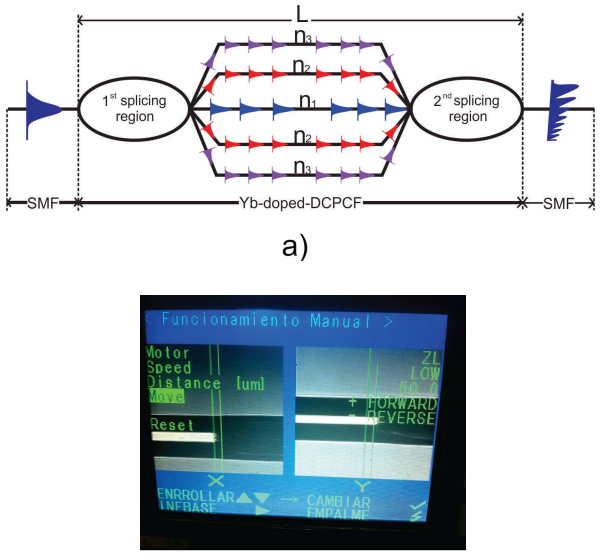

Fig. 1. a) Schematic diagram of the Mach-Zehnder interferometer, b) Image of one collapsed region of one of the splicing region.

TABLE I
SET OF PARAMETERS USED FOR THE SPLICER PROGRAM

Splicer parameter	Value
Arc power	94
Pre-fusion time (ms)	240
Arc duration (ms)	850
Cleaning time (ms)	0

an average separation between the holes of 1μm, and an outer cladding of 125μm (n_3) (See, Inset Fig. 3). Furthermore, as it is shown in Fig. 1b, the core of the SMF input is aligned to the core of the Yb-doped-DCPCF. The SMF|Yb-doped-DCPCF|SMF splicing regions were obtained using a commercial splicer machine (Sumitomo model Type 39) which was programmed with the set of parameters listed in the table 1 which were reported and optimized in [16]. For further reference all modal properties of this Yb-doped-DCPCF were reported in [17].

The principle of operation of the three beam optical path MZI can be explained as follows: when the Yb-doped-DCPCF and SMF are spliced the air holes collapse (Fig. 1b) and act as an optical coupler between the two, while the core and claddings of the Yb-doped-DCPCF act as the MZI arms (Fig. 1a). Hence, when the SMF core mode reaches the first collapsed region, it is diffracted and part of the fundamental mode will be coupled into the core (n_1), inner cladding (n_2), and outer cladding (n_3). Given that this fiber has double cladding, each one will behave as an optical path [16]–[18].

Since the core and the claddings have different effective refractive index, a phase difference depending on the wavelength and the length of the Yb-doped-DCPCF is produced. In our case, the distance between two collapsed regions corresponds to the physical length of the interferometer.

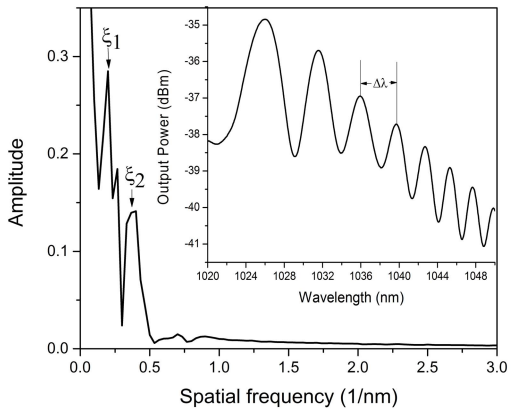

Fig. 2. Spatial frequency analysis of the three optical path MZI.

At the second collapsed region these modes are recombined and at least two main modal interferences occur. The first one is due to the interference between the core mode and a dominant inner cladding mode while the second one is due to the interference between the core mode and a dominant outer cladding modes [16], [18], [19]. The spectral profile of the three optical path MZI is shown in the inset of Fig. 2. Here, it can be seen that the values of the separation between two consecutive peaks does not remain constants. Hence, the spectral response shows an aperiodic sinusoidal waveform [18]. The separation between two consecutive peaks is given by $\Delta\lambda \approx \lambda^2/\Delta n_e L$, where Δn_e is the effective refractive index difference between the two modes involved in the interference pattern, λ represents the wavelength, and L the length of the Yb-doped-DPCF between the two collapsed regions. It can be observed that $\Delta\lambda$ depends both on L and Δn_e. In our experiment the length of the Yb-doped-DCPCF remains constant, however the fiber has two effective refractive indexes differences $(\Delta n_{e_1} = n_{core} - n_{inner})$ and $(\Delta n_{e_2} = n_{core} - n_{outer})$ and as a results different values of the $\Delta\lambda$ were obtained at several wavelengths of the output power (See, Inset Fig. 2) [18]. Finally, the aperiodic sinusoidal curve is different to as expected for an MZI with two optical paths [12]–[15].

In order to determine the components that construct the MZI spectrum, a fast Fourier transform (FFT) was performed (See, Fig. 2) [18], [19]. As it can be observed, the spatial frequency has three dominant peaks due to the presence of the MZI filter which presents different $\Delta\lambda$. Furthermore, the spatial frequency can be expressed as a function of the length and the effective refractive index as shown in the following equation [19], [20]:

$$\xi = \frac{\Delta n_e L}{\lambda^2}, \tag{1}$$

From this equation, it can be derived that the cladding modes are induced because they have higher differential effective index (Δn_e) [20]. Therefore, we can estimate that (ξ_1) is the result of the interference between the core and the inner cladding, and that (ξ_2) results from the interference between the core and the outer cladding. Thus, the outer and

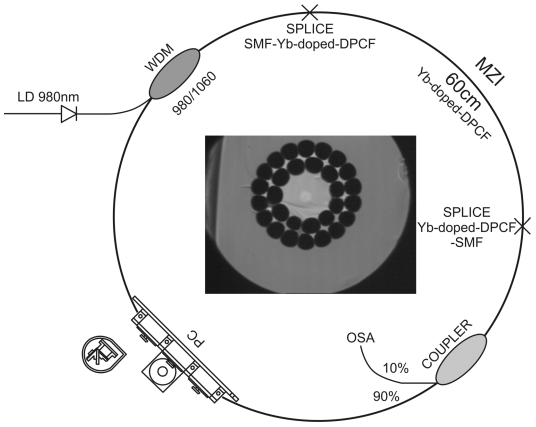

Fig. 3. Experimental setup of the fiber ring laser.

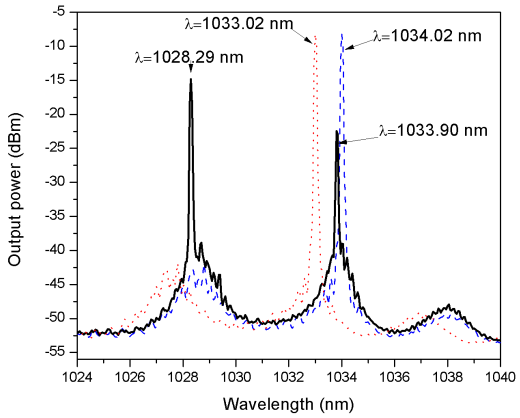

Fig. 4. Laser emissions spectra.

inner cladding and the core of the Yb-doped-DCPCF form a three beam optical path [16], [18], [19].The insertion loss of the three beam optical path MZI was around 12 dB.

III. Laser Setup

The proposed laser consists of a ring cavity (Fig. 3) uses a 60 cm long Yb-doped-DCPCF segment pumped with a laser diode (Thorlabs, Model PL980P330). The laser diode emits at 980 nm with 330 mW maximum output power and is spliced to a wavelength division multiplexer (WDM 980/1060 nm). To carry out our experiments the laser diode was set at 300 mw and a 10 dB 90/10 optical coupler (OC) was used to sample the beam. The 10% output was connected to an optical spectrum analyzer (OSA, Anritsu Model MS9710B) while the 90% power output was used to provide feedback to the laser cavity in order to maintain the laser oscillation. A polarization controller (PC) was used to control the polarization state as shown in Fig.3. The operation of the laser cavity can be controlled by changing the coupling ratio of the OC and the Yb-doped-DCPCF length [14]. A total ring cavity length about of 3 m was obtained

Furthermore, after the first collapsed region, one part of the pumped beam energy will be confined in the doped core fiber, where some of this energy will be transferred to the Yb^{3+} ions. This consequently will allow the amplified spontaneous emission (ASE) to occur. It is important to note that, the laser diode pump emits continuously and the emission wavelength range from 1020-1050nm was achieved. Therefore, in this arrangement the Yb-doped-DCPCF is acting as the gain medium and also as the arms of the MZI simultaneously (Fig. 2). In this way, the MZI with three beam optical paths can be used as wavelength selective filter (WSF), and additionally we can take advantage of the PCFs properties such as wavelength dependent and single mode operation over a wide wavelength range [21].

IV. Experimental Results and Discussion

To carry out our experiments, the laser diode was set at a power of 300 mW. Here, it is important to mention, that emission laser lines depend on the transmission interference spectrum produced by the three optical path MZI. Therefore, to control the line emission positions, it was necessary to shift the MZI spectral pattern, which can be obtained by using a PC to change the polarization states entering into the fiber ring cavity. Here, the polarization states were also adjusted until a homogenous linewidth of the Yb-doped-DCPCF was reduced quite enough to obtain a single laser emission as shown Fig. 4 [22].

In this way, a laser emission centered at 1033.02 nm and with an SMSR around 40 dB was obtained. In order to determine the switching capacity of this laser setup, the PC was adjusted until another laser emission was obtained, in our case this emission line occurred at 1034.02 nm and had an SMSR of 40 dB (fig. 4). These SMSR values are similar to that reported in [10]–[14], and [22], in which, the lasers used an MZI as a WSF. Moreover, to obtain dual wavelength laser emissions, it was necessary to change the polarization states (Fig. 4). For our case, lines centered at 1028.29 and 1033.90 nm were obtained. Here, it is important to draw attention to that during the switching process there is a certain point where two lines overlap in wavelength, producing a single emission line. Moreover, for the dual emission case, the SMSR was approximately 30 dB for the emission centered at 1028.29 and around 20 dB for the emission centered at 1033.02 nm. In order to validate the power stability operation of the laser at room temperature, its spectrum was scanned repeatedly for 30 min at intervals of 2 min (Fig. 5). From these results it can be observed that the variations output power were $\leq$1 dB.

On other hand, some feature of the power lasing characteristics of this Yb-doped-DCPCF at 1033.02 nm were measured. For instance, our laser has a threshold power of 7.5 mW of absorbed pump power and after this power level, the laser power showed a 40% slope efficiency [22] with respect to the absorbed power (Fig. 6). Furthermore, the maximum output lasing power achieved for this configuration was measured to be 9 mW. Here, it is important to mention that efficiency and threshold of a laser generally depends on the fraction of the power that is out-coupled from it, and also for the trade-off between the total cavity losses and the gain. Consequently, our setup shows a compromise between the requirement for a low threshold and a high slope efficiency, but, the splicing

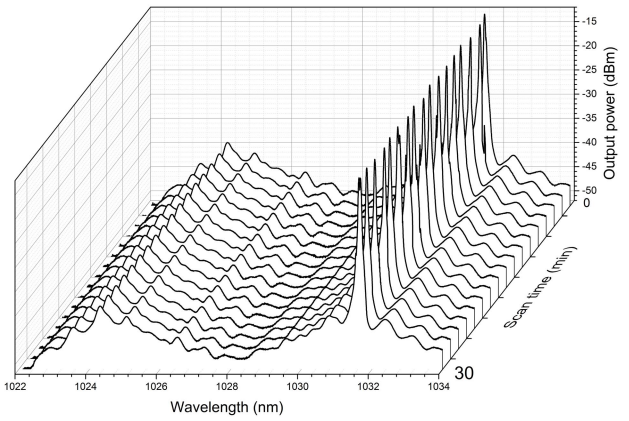

Fig. 5. Measured output spectrum recorded every 2 min.

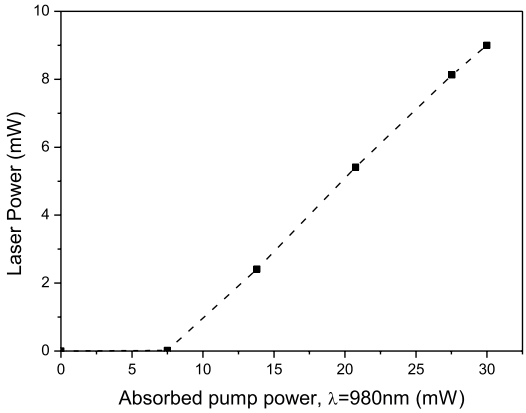

Fig. 6. Slope efficiency of the fiber ring laser.

losses in our Yb-doped-DCPCF resulted to be very high and together with the hand-made cleave facet ends generated excessive losses and subsequently a low slope efficiency. From Fig. 6, it can be noticed that it is possible to convert a larger pump power into more output laser power. In our case, we cannot apply more pump power since we were limited by the laser pump diode used in our experiment. However, our laser setup can be used as a signal seed in an optical amplifier configuration if a larger laser power is required.

V. Conclusions

A ring fiber laser using a single segment of an Yb-doped-DCPCF, which simultaneously acts as the gain medium and the wavelength selective filter, was presented. This is an interesting and convenient configuration since the number of components are reduced simplifying the laser configuration. Moreover, we can switch between a single or a double line emissions by controlling the polarization states. Here, laser emissions were switchable within the range from 1028.29 to 1034.02 nm with a SMSR of 40 dB. Finally, with this simple setup, it was possible to obtain a relatively acceptable laser slope efficiency, however it is expected that this can be significantly improved by optimizing some elements in our system.

References

[1] M. Bashkansky, M. D. Duncan, L. Goldberg, J. P. Koplow, and J. Reintjes, "Characteristics of a Yb-doped superfluorescent fiber source for use in optical coherence tomography," *Opt. Exp.*, vol. 3, no. 8, pp. 305–310, 1998.

[2] P. Gross *et al.*, "Fiber-laser-pumped continuous-wave singly resonant optical parametric oscillator," *Opt. Lett.*, vol. 27, no. 6, pp. 418–420, 2002.

[3] Y. Jeong, J. K. Sahu, R. B. Williams, D. J. Richardson, K. Furusawa, and J. Nilsson, "Ytterbium-doped large-core fibre laser with 272 W output power," *Electron. Lett.*, vol. 39, no. 13, pp. 977–978, 2003.

[4] V. Philippov *et al.*, "High-energy in-fiber pulse amplification for coherent lidar applications," *Opt. Lett.*, vol. 29, no. 22, pp. 2590–2592, 2004.

[5] D. Panasenko, P. Polynkin, A. Polynkin, J. V. Moloney, M. Mansuripur, and N. Peyghambarian, "Er-Yb femtosecond ring fiber oscillator with 1.1-W average power and GHz repetition rates," *IEEE Photon. Technol. Lett.*, vol. 18, no. 7, pp. 853–855, Apr. 1, 2006.

[6] Y. Jeong, J. K. Sahu, D. B. S. Soh, C. A. Codemard, and J. Nilsson, "High-power tunable single-frequency single-mode erbium:ytterbium codoped large-core fiber master-oscillator power amplifier source," *Opt. Lett.*, vol. 30, no. 22, pp. 2997–2999, 2005.

[7] Z. Zhang, L. Zhang, and Z. Xu, "Tunable multiwavelength ytterbium-doped fiber laser based on nonlinear polarization rotation," *J. Nonlinear Opt. Phys. Mater.*, vol. 21, no. 3, p. 1250041, 2012.

[8] Y.-G. Han, S. B. Lee, C.-S. Kim, J. U. Kang, U.-C. Paek, and Y. Chung, "Simultaneous measurement of temperature and strain using dual long-period fiber gratings with controlled temperature and strain sensitivities," *Opt. Exp.*, vol. 11, no. 5, pp. 476–481, 2003.

[9] Y. Zhou, P. C. Chui, and K. K. Y. Wong, "Multiwavelength single-longitudinal-mode ytterbium-doped fiber laser," *IEEE Photon. Technol. Lett.*, vol. 25, no. 4, pp. 385–388, Feb. 15, 2013.

[10] W. Guan and J. R. Marciante, "Dual-frequency operation in a short-cavity ytterbium-doped fiber laser," *IEEE Photon. Technol. Lett.*, vol. 19, no. 5, pp. 261–263, Mar. 1, 2007.

[11] C. Tu, W. Guo, Y. Li, S. Zhang, and F. Lu, "Stable multiwavelength and passively mode-locked Yb-doped fiber laser based on nonlinear polarization rotation," *Opt. Commun.*, vol. 280, pp. 448–452, Dec. 2007.

[12] C. Tu, W. Guo, Y. Li, S. Zhang, H. Zhu, and F. Lu, "Multiwavelength Yb-doped fiber ring laser based on a Mach–Zehnder interferometer," *Microw. Opt. Technol. Lett.*, vol. 50, no. 3, pp. 723–725, 2008.

[13] L. V. Nguyen, D.-S. Hwang, D. S. Moon, and Y. Chung, "Tunable comb-filter using thermally expanded core fiber and ytterbium doped fiber and its application to multi-wavelength fiber laser," *Opt. Commun.*, vol. 281, no. 23, pp. 5793–5796, 2008.

[14] M. R. A. Moghaddam, S. W. Harun, S. Shahi, K. S. Lim, and H. Ahmad, "Comparisons of multi-wavelength oscillations using Sagnac loop mirror and Mach–Zehnder interferometer for ytterbium doped fiber lasers," *Laser Phys.*, vol. 20, no. 2, pp. 516–521, 2010.

[15] Y. Meng *et al.*, "Tunable double-clad ytterbium-doped fiber laser based on a double-pass Mach–Zehnder interferometer," *Opt. Laser Eng.*, vol. 50, no. 3, pp. 303–307, 2012.

[16] J. M. Sierra-Hernandez *et al.*, "Torsion sensing setup based on a three beam path Mach–Zehnder interferometer," *Microw. Opt. Technol. Lett.*, vol. 57, no. 8, pp. 1857–1860, 2015.

[17] J. K. Sahu *et al.*, "Jacketed air-clad cladding pumped ytterbium-doped fibre laser with wide tuning range," *Electron Lett.*, vol. 37, no. 18, pp. 1–2, 2001.

[18] E. Huerta-Mascotte *et al.*, "A core-offset Mach Zehnder interferometer based on a non-zero dispersion-shifted fiber and its torsion sensing application," *Sensors*, vol. 16, no. 6, p. 856, 2016.

[19] Z. Zhao *et al.*, "All-solid multi-core fiber-based multipath Mach–Zehnder interferometer for temperature sensing," *Appl. Phys. B*, vol. 112, no. 4, pp. 491–497, 2013.

[20] L. V. Nguyen, D. Hwang, S. Moon, D. S. Moon, and Y. Chung, "High temperature fiber sensor with high sensitivity based on core diameter mismatch," *Opt. Exp.*, vol. 16, no. 15, pp. 11369–11375, Jul. 2008.

[21] P. S. J. Russell, "Photonic-crystal fibers," *J. Lightw. Technol.*, vol. 24, no. 12, pp. 4729–4749, Dec. 2006.

[22] J. T. Ahn, H. K. Lee, K. H. Kim, M.-Y. Jeon, D. S. Lim, and E.-H. Lee, "A stabilised fibre-optic Mach–Zehnder interferometer filter using an independent stabilisation light source," *Opt. Commun.*, vol. 157, nos. 1–6, pp. 62–66, 1998.